High-resolution seismic imaging of the Sohagpur Gondwana basin, central India: Evidence for syn-sedimentary subsidence and faulting

K Dhanam*, P Senthil Kumar, D Mysaiah, P Prabhakara Prasad and T Seshunarayana

National Geophysical Research Institute, Council of Scientific and Industrial Research, Uppal Road, Hyderabad 500 606, India.

**Corresponding author. e-mail: dhanamk6@gmail.com*

Gondwana sedimentary basins in the Indian Shield preserve a rich record of tectonic, sedimentary and volcanic processes that affected Gondwanaland. The Gondwana rocks were deposited in the linear rift basins that were formed during Permian–Cretaceous time, similar to their neighbours in Australia, Africa and Antarctica. In this study, we illustrate how Gondwana tectonics affected the Sohagpur Gondwana basin that occurs at the junction of the Mahanadi and Son–Narmada rift systems in the central India, through a high-resolution seismic reflection study along six profiles, covering the central part of the Sohagpur basin. The study reveals (1) ∼1000 m thick, gently dipping Barakar Formation, (2) thick coal seams at a depth of 350–550 m, and (3) NNW–SSE to NW–SE striking steeply dipping normal faults defining rift geometry. These results indicate that the Sohagpur basin contains a thick Lower Gondwana sedimentary succession with a high potential of coal resources and were affected by extensional tectonics. The rift structure in the study area is a syn- to post-sedimentary deformational structure that was formed arguably in response to tectonics that pervasively affected Gondwanaland.

1. Introduction

Gondwana supercontinent broke at ∼200–160 Ma, rifted and the fragments drifted away in many directions (McLoughlin 2001; Riley and Knight 2001; Conrad and Gurnis 2003; Jokat *et al.* 2003). One of the fragments – the Indian Shield, drifted approximately northward and eventually collided onto the Eurasian plate, producing the spectacular trans-continental Himalayan fold-thrust belt (Norton and Sclater 1979; Reeves and de Wit 2000; Reeves *et al.* 2004; Melluso *et al.* 2009). The break-up and northward journey immensely affected the Indian Shield in several ways (e.g., Veevers and Tewari 1995; Biswas 1999; Veevers 2009), including erosion of the base of its lithosphere (e.g., Kumar *et al.* 2007) and development of several structural basins (e.g., Acharyya and Lahiri 1991). Before the break-up, Gondwana supercontinent developed many sagging sedimentary basins along the palaeo-suture zones (mostly Proterozoic mobile belts along which adjoining cratons were juxtaposed), at the end of Carboniferous. A thick succession of sedimentary rocks piled up in these basins. The supercontinental break-up and rifting immensely affected these basins, producing several intra-continental rift structures, which again served as locales of sedimentation in association with continued tectonic activity (e.g., Biswas 1999; Veevers 2009). The peninsular Indian

Keywords. Sohagpur Gondwana basin; high resolution seismic reflection survey; coal beds; faults.

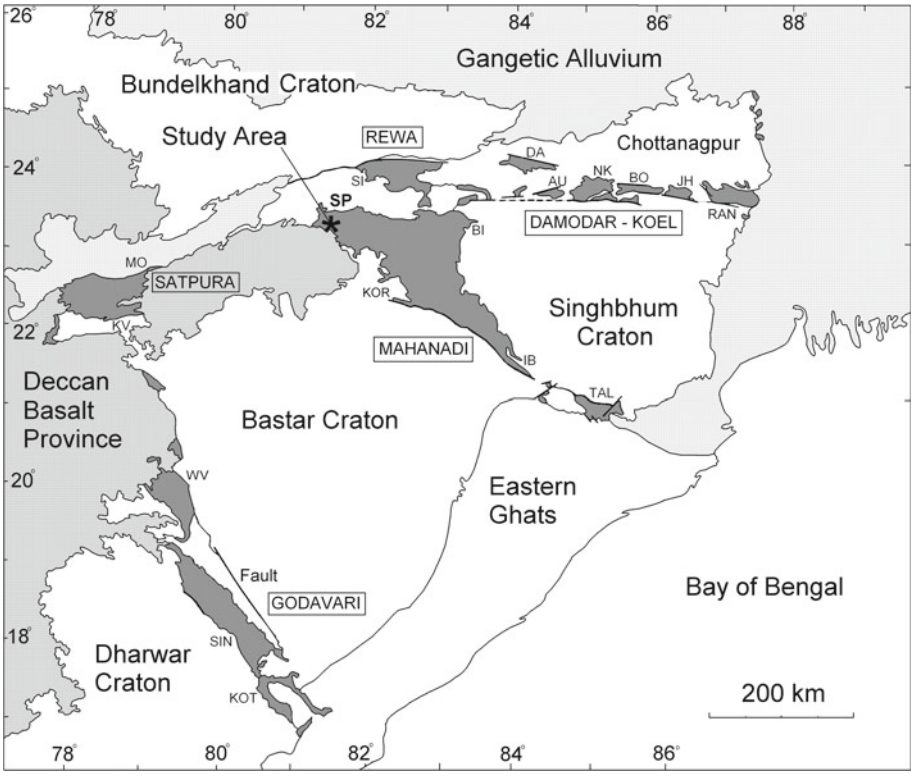

Figure 1. Geological map of the peninsular India showing the distribution of Gondwana sedimentary basins, shown in dark grey colour (after Veevers and Tewari 1995). These sedimentary basins are bound by rift zones that were formed between the Archaean cratons such as Dharwar, Bastar and Singhbhum. The Deccan Traps overlie the Gondwana sedimentary rocks. Abbreviations of different coal fields are: AU – Auranga, BO – Bokaro, BI – Bisrampur, DA – Daltonganj, IB – Ib River, JH – Jharia, KOR – Korba, KOT – Kothagudem, KV – Kanhan Valley, MO – Mohpani, NK – North Karanpura, RAN – Rani, SI – Singrauli, SIN – Singreni, TAL – Talcher, WV – Wardha Valley. The present study area is the Sohagpur basin, which is a part of the Rewa basin.

Shield contains many such linear belts of Gondwana sedimentary rocks, which are known as Gondwana Supergroup, occurring in the Son–Narmada, Rajamahal–Purnea, Rewa, Satpura, Mahanadi and Godavari basins (figure 1). Continuity of the structure and lithological make-up of the Godavari and Mahanadi basins are now present in Antarctica (see Veevers 2009).

The Indian Gondwana basins contain a rich record of tectonic, sedimentary and volcanic history of Gondwanaland (e.g., Lisker and Fachmann 2001; Biswas 2003). Our present study area is Sohagpur basin, which shares the boundary with the Rewa basin in the north and the Mahanadi basin in the southeast. It is located at the junction of two major rift systems (Son–Narmada and Mahanadi). Previous studies have shown that the Sohagpur basin contains a thick succession of Gondwana Supergroup (Raja Rao 1983), which is cut by E–W trending normal faults (Pareek 1987). Recently, we carried out a high-resolution seismic reflection study in the central part of the Sohagpur basin (figure 2) that brought out new geophysical information on the nature of coal-bearing sedimentary rocks and new rift structures, which are presented in this paper. The seismic method used high-frequency seismic waves (>80 Hz), which were reflected from the shallow horizons, and resolved small-scale geological features in the form of several reflectors (e.g., Gochioco and Cotten 1989; Sheriff 1991). The vertical resolution of the reflectors is approximately one-fourth of the wavelength of the seismic waves (Widess 1973). The present study provides a depth resolution of 5 m, which depends on the interval velocity of 2000 m/s (obtained from the borehole sonic-log data) and the predominant reflector frequency of 100 Hz. In this paper, we present the results of seismic survey and discuss their significance in deciphering the tectono-sedimentary processes that affected the Sohagpur basin.

2. Study area

The Sohagpur basin is a part of the large sediment-filled trough in the drainage basin of the Son River. Geology of the basin was described by Raja Rao (1983) and Pareek (1987). The Sohagpur basin is

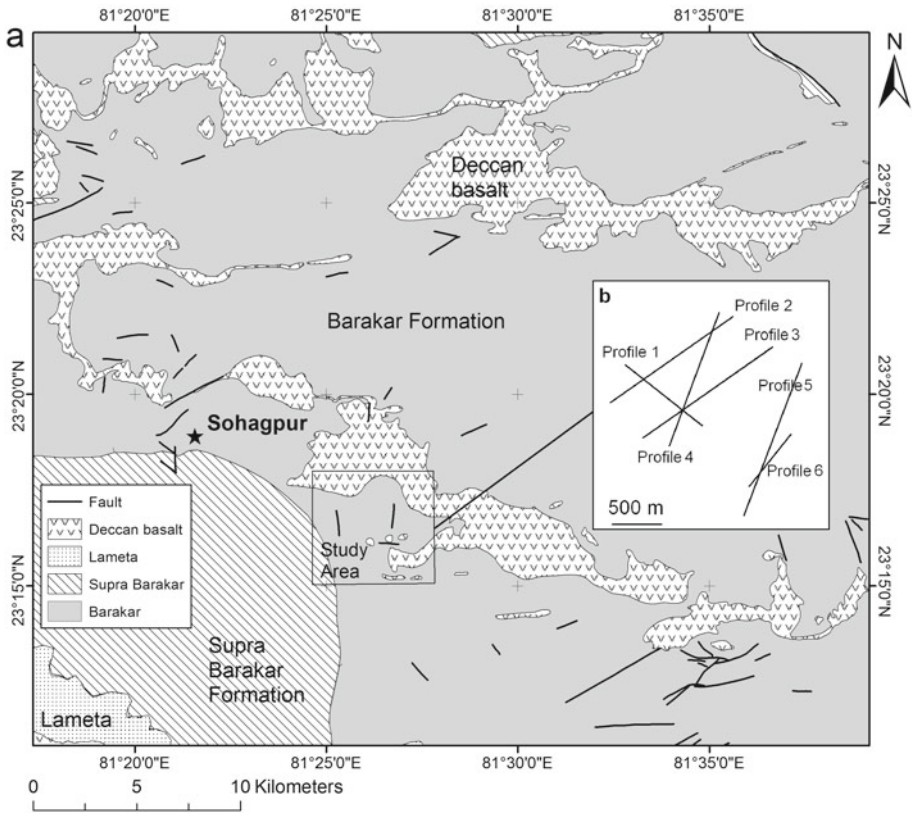

Figure 2. (**a**) Geological map of the study area and (**b**) the location of the seismic profiles (after Raja Rao 1983). Note the presence of two NW–SE faults and one NNW–SSE fault in the study area.

composed of thick sedimentary strata that unconformably overlie the Precambrian basement rocks, dominantly made up of pink porphyritic gneiss. The sedimentary rocks of the Gondwana Supergroup strike WNW–ESE to E–W and dip up to 5° towards north (Pareek 1987). The area is traversed by a major en-echelon ENE–WSW-trending fault with down-throw towards the north, runs through the middle of the Sohagpur coalfield, along its southern boundary (Pareek 1987). The rocks of the Talchir Formation (Upper Carboniferous–Lower Permian) unconformably overlie the basement; it contains shale, siltstone and boulder beds, with some marine fossils. The overlying Barakar Formation (Lower Permian) is composed of sandstones with bands of shale, carbonaceous shale and coal seams. The formation is approximately 450 m thick and subdivided into three members, of which the middle one is the thickest. The lower member contains a greyish-white feldspathic garnetiferous sandstone, siltstone and shale, and is devoid of coal seams. The middle member includes cross-bedded feldspathic sandstones with garnet, and thick workable coal seams in the lower portion. Ferruginous sandstones, shales, and siltstones characterize the upper unit.

The Pali Formation (Triassic) that overlies the Barakar Formation is approximately 350 m thick, and contains three members. The lower member comprises coarse-grained sandstones and shales. The middle member contains coal bearing medium- to fine-grained sandstones, shales, and carbonaceous shales. The Parsora Formation (Upper Triassic) occurs in the northern part of the basin and comprises coarse-grained to pebbly ferruginous sandstones and shales. The succeeding Lameta Beds (Upper Cretaceous) include greenish and reddish, poorly consolidated sandstones and shales with nodular limestone at the top. A marked unconformity separates the Lameta Beds from the Parsora Formation. The Sohagpur coalfield is profusely intruded by dykes and sills (Deccan Trap, Upper Cretaceous–Eocene), and dolerites are also emplaced along the fault (Sarkar and Singh 2005; Sheth *et al.* 2009). The study area largely exposes the Barakar Formation overlain by the exposures of Supra–Barakar Formation and Deccan Traps in the south and north, respectively (figure 2b).

3. Seismic data acquisition and processing

The high-resolution seismic reflection data were acquired along six profiles as shown in figure 2(b). The selection of the optimum data acquisition geometry, receiver (geophones) and recording

parameters was made in the field after analysis of the walkaway noise test (e.g., Vincent *et al.* 2006). The quality of the high-resolution seismic data depends mainly on the data acquisition geometric parameters (e.g., Ziolkowski and Lerwill 1979; Knapp and Steeples 1986a) and the energy source (e.g., Miller *et al.* 1994). In the present study, we employed a common depth point (CDP) technique that incorporated an end-on shooting geometry (e.g., Knapp and Steeples 1986b; Gochioco and Kelly 1990; Tselentis and Paraskevopoulos 2002) with a geophone interval of 5 m, and a shot point interval of 10 m. The near and far offsets were 150 and 445 m, respectively. Each receiver station was composed of a group of 10 geophones of 10 Hz frequency. Geometrics 60-channel seismograph was used to record the seismic data. Each seismic record (shot gather) was composed of 60 channels. A maximum record length of 2 s and a sample interval 0.25 ms were chosen. The recording geometry provides a nominal CMP fold of 15.

In the seismic data processing, first, the seismic data acquisition parameters (geometry building) were applied to the seismic records. High amplitude noise, polarity reversals and the signals related to the direct and refracted waves in the data were eliminated. Elevation statics were applied to correct the effect of topography and near-surface heterogeneity such as weathering. Power function was used for spherical divergence correction (VT) to retrieve the lost amplitude in the data. The dominant ground roll present in the data was removed using the band pass filter (figure 3a) (30–150 Hz) and the frequency-wave number filter also applied on shot gather to enhance the signal-to-noise ratio (Ziolkowski and Lerwill 1979; Arun *et al.* 2011). Figure 3(b) shows the band limited spiking-deconvolution input and output, using

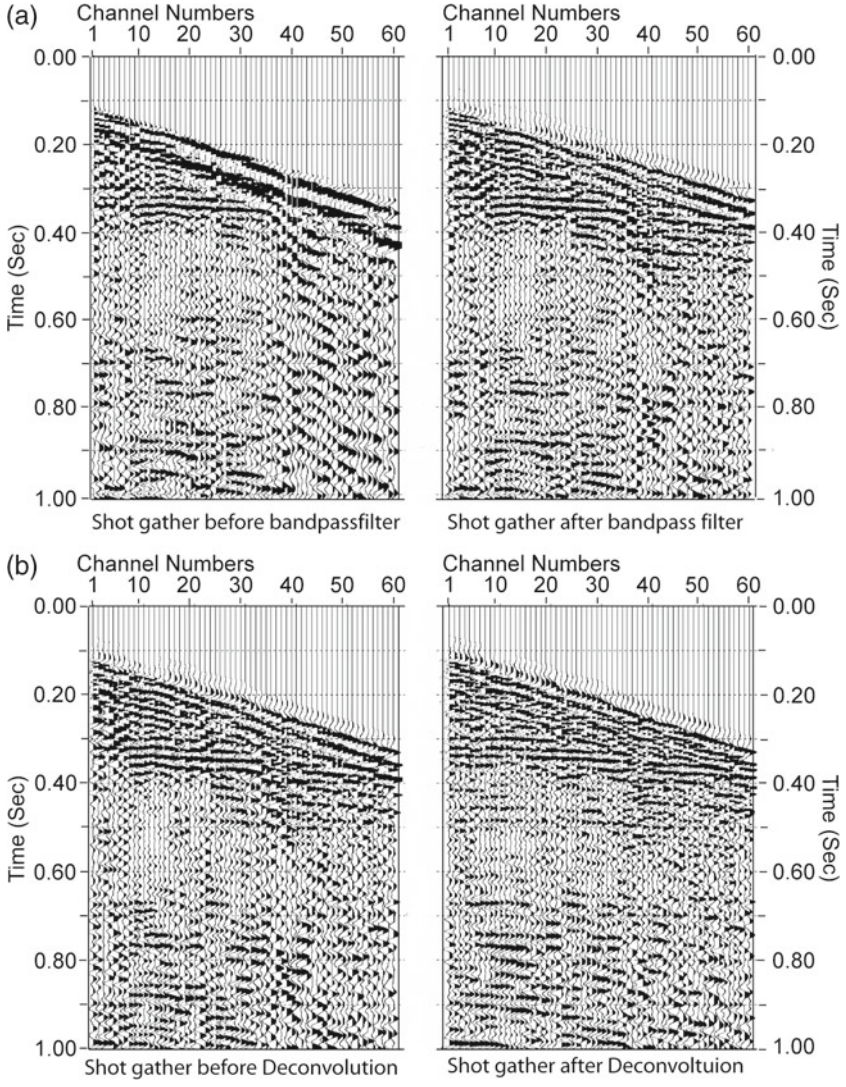

Figure 3. (**a**) Shot gathers before and after application of bandpass filter and (**b**) shot gathers before and application of band limited spiking-deconvolution.

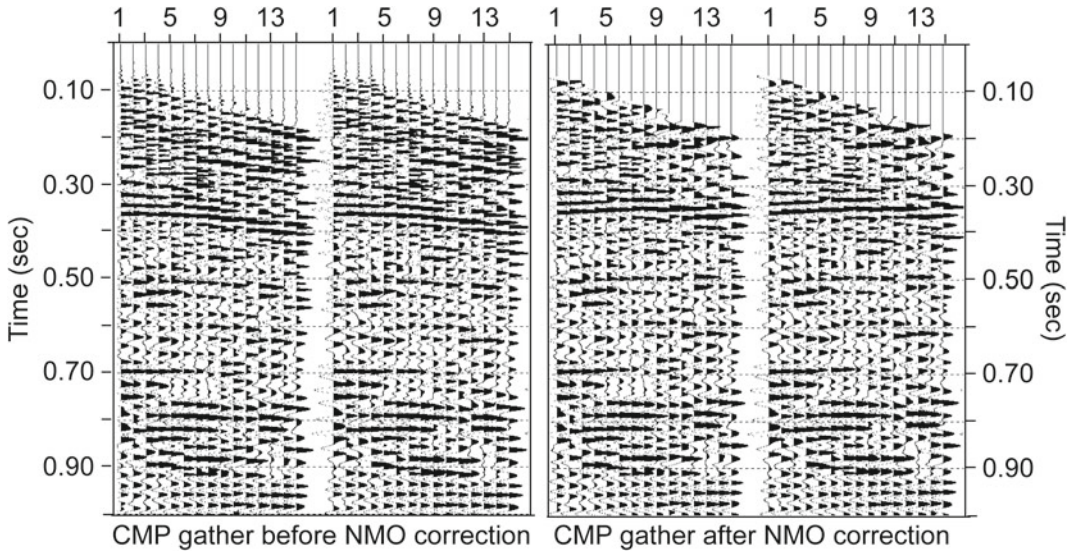

Figure 4. CMP gathers before and after application of normal-moveout correction.

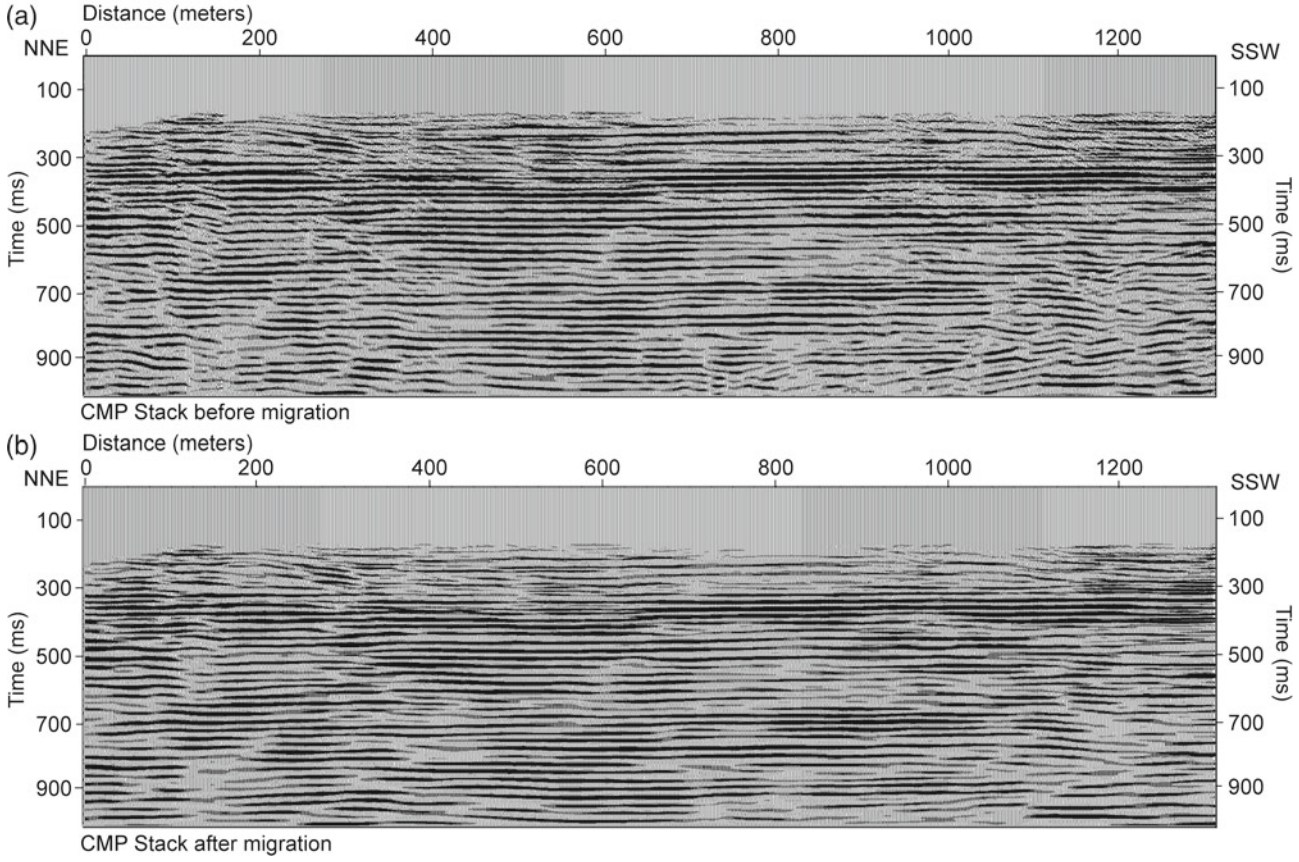

Figure 5. (**a**) Final CMP stack section and (**b**) seismic section with Kirchhoff time migration.

operator length 80 m to improve the vertical resolution by compressing the wavelet of the seismic data with improved frequency bandwidth (Peter Cary 2006). The data were converted to common midpoint (CMP) gathers. The primary velocity analysis was carried out using the CMP gathers based on best alignment of normal-moveout corrected data and quality of stacking. The final velocity analysis was performed again after the residual static corrections. The final stacking velocity was used for normal-moveout correction (figure 4) and these gathers were used in the stacking. The

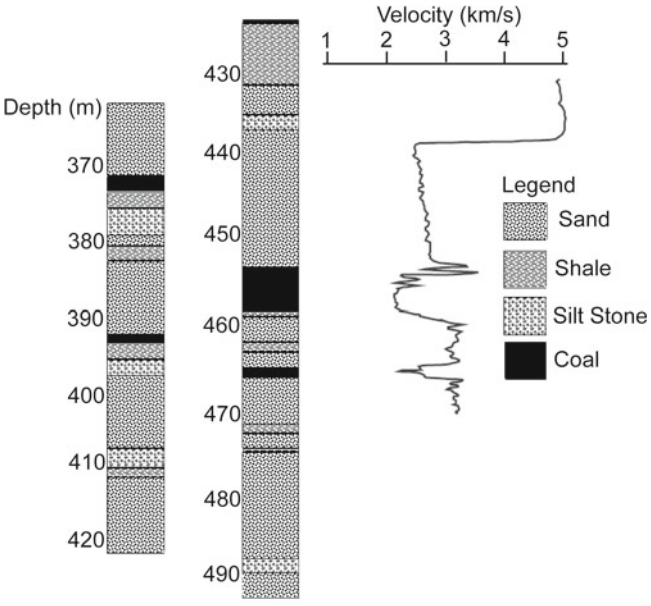

Figure 6. Borehole (BH-1) lithology and interval velocities from sonic the log.

random noise was suppressed by F-X deconvolution (Bekara and Van der Baan 2009) and time varying band pass filter was also applied for further improvement. Post-stack Kirchhoff migration (time) was applied to collapse the diffracted energy and correct dip events (Gray *et al.* 2001). The final stack and time migrated seismic sections were shown in figure 5(a and b). The time sections were converted into depth sections using interval velocities guided by the borehole lithology and sonic log data (figure 6). The final processed seismic reflection sections are shown in figures 7 and 8.

4. Results

Figures 7 and 8 show the seismic sections of the six profiles. The estimated arrival time of seismic waves in all seismic sections is about 0.6 s that correspond to a depth of 1000 m. Figure 7(a) is the seismic section of profile 1. Length of the profile is 830 m; direction of the profile is NW–SE. The seismic section shows several weak-to-strong reflectors. The strong reflections are present at a depth range of 400–550 m. Some of them are making different apparent dips of ∼6°, 3° and 17°. No significant disturbance due to faulting is observed in this seismic section. However, the changes in the dip of reflectors at different depth levels are attributed to the variations in the depositional structures.

Figure 7(b) is the seismic section of profile 2. Length of the profile is 1340 m; direction of the profile is NE–SW. The strong reflectors of varying thickness at a depth range of 350–500 m are observed. The seismic reflectors show apparent dips of ∼5° and 6° pertaining to the sedimentary structures. Disturbances in the amplitude of seismic reflectors are observed at two places, where a trace of a normal fault F2A is detected at a distance of 200 m from the NE end with a dip of 83° towards northeast; another normal fault F1A is encountered at 700 m with a dip of 79° towards southwest. These two faults dip away from each other.

Figure 7(c) is the seismic section of profile 3. Length of this profile is 1400 m. Direction of the profile is NNE–SSW. The strong reflectors at a depth of 400–550 m indicate the presence of coal seams, as observed in the borehole (see figure 6). The seismic reflectors show apparent dips of 2° to 4°. A major disturbance was observed at a distance of 200 m from the NNE, where the seismic amplitude changes, which is interpreted to be a trace of a northerly dipping normal fault F2A with a dip of 82°. Another southerly dipping fault (F1B) is observed about 750 m away from the NNE end of the profile; this fault shows strong displacement in the intermediate depth level. Dip of this fault is 85° towards SSW. The fault F1B is related to F1A in the profile 2. The fault F2A is same as that of seen in the profile 2, as these two profiles intersect at the fault. It is interesting to note that the fault F1B is present only in the middle to lower parts and it does not seem to displace the sedimentary layers in the upper levels. Therefore, these structures are interpreted to have formed by syn-sedimentational faulting.

Figure 7(d) is the seismic section of profile 4. Profile 4 is parallel to the profile 2 (figure 9). Length of the profile is 1370 m. Direction of the profile is NE–SW. The strong reflectors at a depth range of 350–550 m indicating the presence of coal seams. The seismic reflectors show apparent dips of 3° and 4°. A major disturbance is observed at a distance of 100 m from NE, where the seismic amplitude changes, and is interpreted to be a trace of a normal fault F3A with a dip of 80° towards southwest. Another fault F2B with a dip of 84° towards northeast is detected at a distance of 450 m. The faults F3A and F2B together provide a rift geometry. The F2B also corresponds to the fault F2A in the profiles 2 and 3. The varying reflector thickness across the faults may be due to syn-sedimentational subsidence, as the rate of sedimentation changes across the fault, which causes the variation in the bed thickness (Childs *et al.* 2003).

Figure 8(a) is the seismic section of profile 5. Length of the profile is 1330 m. Direction of the profile is NNE–SSW. The strong horizontal reflectors at a depth range of 350–550 m indicate subhorizontal coal seams. A disturbance in the seismic

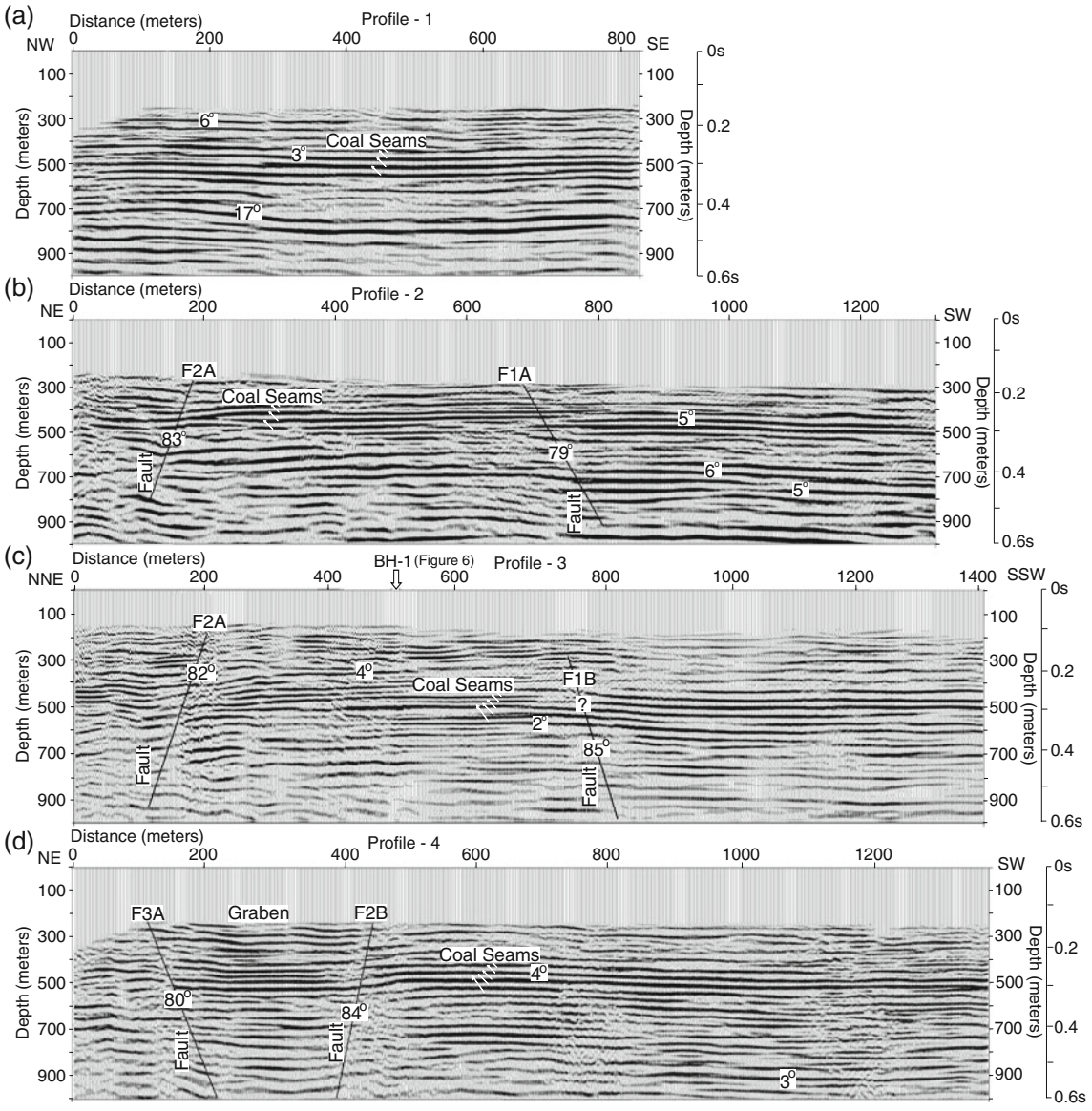

Figure 7. High-resolution seismic reflection sections of profiles 1, 2, 3 and 4.

reflectors is observed at a distance of 250 m from NNE end, which is due to the trace of a normal fault F3B with a dip of 74° towards SSW. The fault F3B corresponds to the fault F3A in the profile 4. In the seismic section, the Deccan Traps are also observed up to a depth of 350 m over a distance of 400 m from the NNE end. The fault F3B cuts across the Deccan Traps. Another fault F4 is detected at a distance of 100 m from NNE end; dip of the fault is 83° towards SSW. Figure 8(b) is the seismic section of the profile 6. Length of the profile is 660 m. Direction of the profile is NE–SW. The prominent near horizontal reflectors are observed at a depth range of 400–500 m, indicating the coal seams. There is no significant disturbance due to faulting observed.

We prepared the seismic sections in three dimensions (3D). The 3D sections show a good continuity of reflectors at the intersecting seismic sections. Figure 9 provides a fault network model based on the traces of fault planes observed at different seismic sections. It contains three normal faults, 1, 2 and 3. The fault 1 is noticed in the profiles 2 and 3 and is absent in other seismic sections. Strike and dip of this fault is 80°N and 81°W, respectively. The fault 2 is observed in the profiles 2, 3 and 4, it strikes 45°N and dips 79°W, and this fault appears to terminate between the profiles 4 and 5. The fault 3 is seen in the profiles 4 and 5; it strikes 25°N and dips 77°W. The faults 2 and 3 provide an asymmetric rift geometry. Based on the apparent dips of reflectors observed between the profiles 1 and 2,

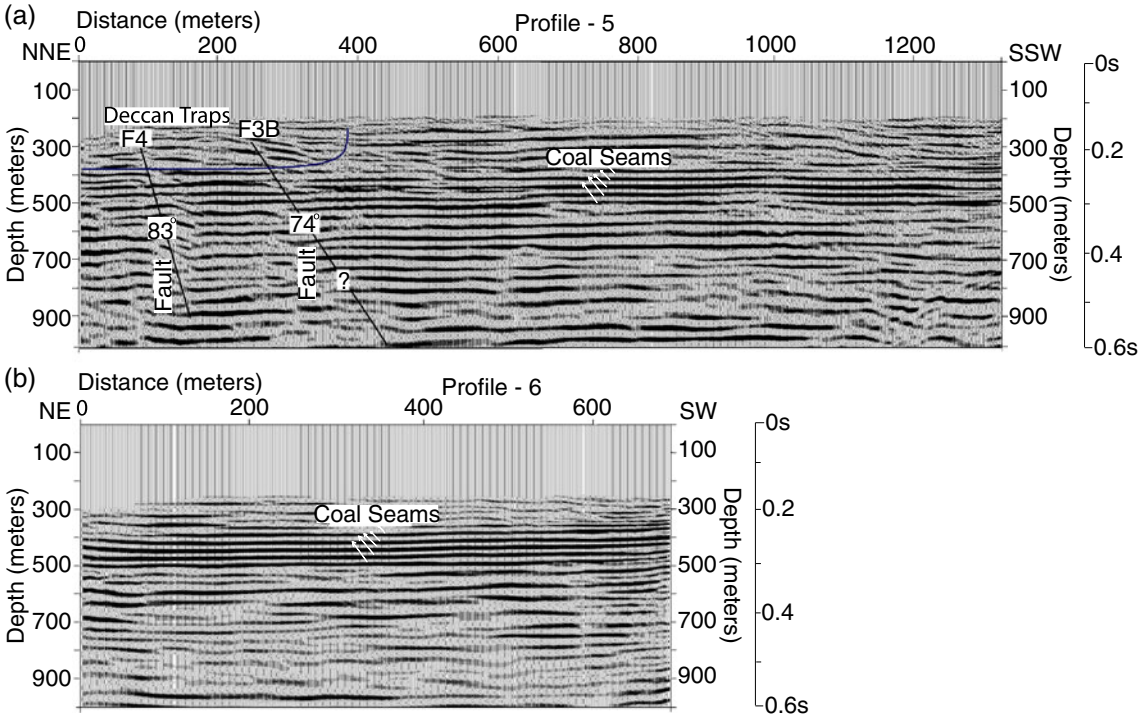

Figure 8. High-resolution seismic reflection sections of profiles 5 and 6.

and 1 and 3, we calculated their true dips, which is 5° towards N, 80°E. It corresponds to the geometry of sedimentary bedding planes in the study area. Interestingly, the previous work also noticed a dip value of 5° towards north (Pareek 1987). Although our study finds similar dip values, the difference in the dip direction can be attributed to the tectonic disturbance or variation in the depositional surface. The present study also shows a 200 m thick subhorizontal strong reflector zone at a depth range of 350–550 m from the surface. This zone corresponds to the coal seams found at a depth of 371, 393, 422, 454 and 465 m, having a thickness of 2, 0.5, 0.3, 5 and 1 m, respectively, as observed in the cored borehole (BH-1) that was drilled in the profile 3 (figure 9).

5. Discussion

The present seismic study establishes three normal faults; two in NW–SE directions (faults 1 and 2) and the other (fault 3) in NNW–SSE direction (figure 9). Although the geological map (figure 2) shows the presence of two E–W and a N–S trending fault in the study area, these are not reflected in the seismic profiles. On the other hand, the seismic sections show new faults that cannot be mapped through surface geological mapping as these are syn-sedimentary faults that do not intersect the surface. Therefore, these faults are new additions to the geologic map of the study area (figure 2).

The NW–SE to NNW–SSE normal faults can thus be related to the formation of NW–SE oriented Mahanadi rift system and its reactivation in the study area (figure 1). The normal faults in the study area would thus indicate the interaction of tectonic processes that affected Mahanadi rift zone. Similar to the Godavari rift zone that terminates against the Narmada–Son rift zone (e.g., Biswas 2003), the Mahanadi rift zone should terminate at the Sohagpur basin, where it meets the ENE–WSW trending Naramada–Son rift zone (figure 1).

The faults in the Barakar Formation indicate the syn-sedimentational subsidence in the Sohagpur basin. Although the fault 1 disrupts the Barakar Formation, the sedimentary layers in the upper level partially bury them (figure 6d). This is an example of syn-sedimentational fault, supporting the view that Gondwana sedimentation took place in an active tectonic environment (see Biswas 1999). Chakraborty and Ghosh (2005) have shown the Satpura basin as a pull-apart tectonic basin, where fault-controlled synsedimentary subsidence occurred. However, we do observe the faults completely disrupting the entire succession as seen in figure 7(a–c). Hence, the present study provides evidence for both syn- and post-depositional faulting, and thus representing the tectonic activity of Permian time, when the Indian continent was a part of Gondwanaland, in which Antarctica was juxtaposed along the eastern Indian continental margin (Veevers 2009). The Mahanadi rift zone was

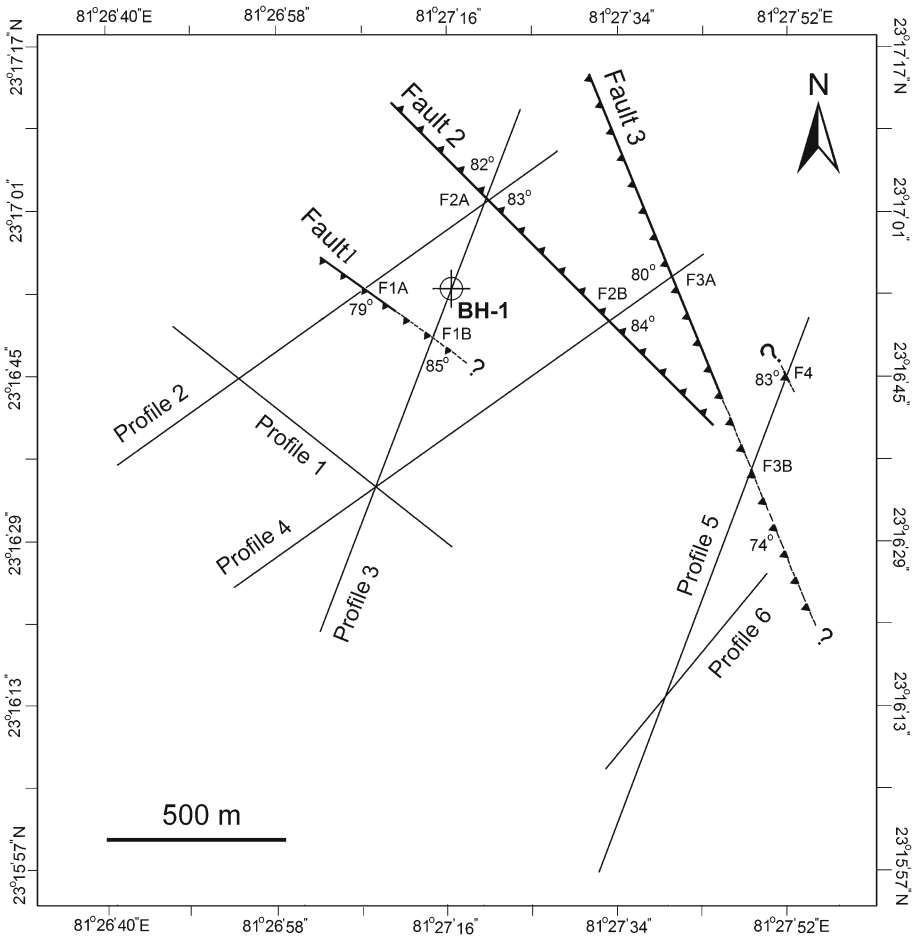

Figure 9. Distribution of faults at a depth of 300 m delineated by the present seismic study. The deep borehole (BH-1) was drilled in profile 3, and was used to validate the results of the seismic study.

an integral part of the Lambert rift zone of Antarctica until the break-up and drifting that separated India and Antarctica in Cretaceous. The Permian sedimentary rocks in the Sohagpur and Mahanadi basins were derived from the Precambrian basement in the central India, the Eastern Ghats granulite belt and those regions around the Lambert rift, as shown by the palaeo-current directions and the geochronologic data (e.g., Veevers and Tewari 1995; Veevers 2009).

The present seismic study also delineates coal bearing sedimentary layers at a depth range of 350–550 m, which has been further confirmed by the drilling results. A recent drilling by an industry has shown the presence of coal-bed methane in this area (Sundaram 2007). A further study with a scope to understanding the thermal evolution of the sedimentary basin is essential to assess the occurrence of coal-bed methane deposits in the basin. The basement rocks of the Gondwana sedimentary rocks are also rich in heat producing elements such as K, U and Th (e.g., Senthil Kumar *et al.* 2007a, b, 2009) and are responsible for high heat flow observed in these belts (e.g., Rao and Rao 1983). Sarkar and Singh (2005) have shown the heat flow density values ranging from 85 to 90 mWm^{-2}. These values are much higher than those observed in the cratonic areas, where heat flow is found to vary from 30 to 50 mWm^{-2} (e.g., Senthil Kumar and Reddy 2004). High-heat flow in the presence of suitable subsidence history would aid in the formation of oil and gas in these basins. A recent thermo-chronologic study in the Mahanadi basin indicates multiple episodes of tectonic and metamorphic events in the time window of 443–119 Ma (Lisker 2004). The new faults in the study area could be attributed to the tectonic processes that affected the Mahanadi basin in that time window. Thus, our study confirms the extensional tectonics in the Sohagpur basin, which probably a local reflection of a global tectonic event that affected Gondwanaland during Permian time.

6. Conclusions

The present study provides high-resolution seismic images of the Sohagpur basin and the fault systems

present in them. These images show about 200 m thick zone of strong reflections pertaining to coal seams at a depth of 350–550 m. These images also provide, for the first time, the geophysical evidence for the NW–SE to NNW–SSE oriented graben in the Sohagpur basin, indicating the northwestward continuation of Mahanadi rift structure up to the present study area. These faults have characteristics of both syn- and post-depositional faulting and thereby indicating the tectonic and sedimentary processes that affected Gondwanaland during Permian time.

Acknowledgements

The authors thank members of the Engineering Geophysics Division for support in the field data acquisition; Reliance Industries Limited for the financial support; Director, NGRI for encouragement and permission to publish this paper. They also thank the anonymous reviewer and the Associate Editor for the constructive comments, which significantly improved the manuscript.

References

Acharyya S K and Lahiri T C 1991 Cretaceous palaeogeography of the Indian subcontinent; A review; *Cret. Res.* **12** 3–26.

Arun K A, Bharat C J and Narinder P S 2011 The role of statics application in the image of sub-surface in fold belt areas: Extended abstract presented at GEO-India, Greater Noida, New Delhi, India, January 12–14, 2011.

Bekara M and Van der Baan M 2009 Random and coherent noise attenuation by empirical mode decomposition; *Geophysics* **74** V89–V98, doi: 10.1190/1.3157244.

Biswas S K 1999 A review on the evolution of rift basins in India during Gondwana with special reference to western Indian basins and their hydrocarbon prospects; *Proc. Indian Natl. Sci. Acad., Part-A* **65** 261–283.

Biswas S K 2003 Regional tectonic framework of the Pranhita–Godavari basin, India; *J. Asian. Earth. Sci.* **21** 543–551.

Chakraborty C and Ghosh S K 2005 Pull-apart origin of the Satpura Gondwana basin, central India; *J. Earth. Syst. Sci.* **114** 259–273.

Childs C, Nicol A, Walsh J and Watterson J 2003 The growth and propagation of synsedimentary faults; *J. Struct. Geol.* **25** 633–648.

Conrad C P and Gurnis M 2003 Seismic tomography, surface uplift, and the breakup of Gondwanaland: Integrating mantle convection backwards in time; *Geochem. Geophys. Geosyst.* **4(3)** 1031, doi: 10.1029/2001GC000299.

Gochioco L M and Cotten S 1989 Locating faults in underground coal mines using high-resolution seismic reflection techniques; *Geophysics* **54** 1521–1527.

Gochioco L M and Kelly J I 1990 High-resolution seismic survey to map paleochannels in an underground coal mine; *Can. J. Expl. Geophys.* **26** 87–93.

Gray S, Etgen J, Dellinger J and Whitmore D 2001 Seismic migration problems and solutions; *Geophysics* **66(5)** 1622–1640, doi: 10.1190/1.1487107.

Jokat W, Boebel T, Konig M and Meyer U 2003 Timing and geometry of early Gondwana breakup; *J. Geophys. Res.* **108**(B9) 2428, doi: 10.1029/2002JB001802.

Knapp R W and Steeples D W 1986a High-resolution common-depth-point seismic reflection profiling: Field acquisition parameter design; *Geophysics* **51** 283–294.

Knapp R W and Steeples D W 1986b High-resolution common-depth-point seismic reflection profiling: Instrumentation; *Geophysics* **51** 276–282.

Kumar P, Yuan X H, Kumar M R, Kind R, Li X Q and Chadha R K 2007 The rapid drift of the Indian tectonic plate; *Nature* **449** 894–897.

Lisker F 2004 The evolution of the geothermal gradient from Lambert Graben and Mahanadi Basin – A contribution to the Indo-Antarctic rift debate; *Gondwana Res.* **7** 363–373.

Lisker F and Fachmann S 2001 Phanerozoic history of the Mahanadi region, India; *J. Geophys. Res.* **106** 22,027–22,050.

McLoughlin Stephen 2001 The breakup history of Gondwana and its impact on pre-Cenozoic floristic provincialism; *Aust. J. Bot.* **49** 271–300.

Melluso L, Sheth H C, Mahoney J J, Morra V, Petrone C M and Storey M 2009 Correlations between silicic volcanic rocks of the St Mary's islands (southwestern India) and eastern Madagascar: Implications for Late Cretaceous India–Madagascar reconnection; *J. Geol. Soc. London*, **166** 283–294.

Miller R D, Pullant S E, Steeples D W and Hunter J A 1994 Field comparison of shallow P-wave seismic sources near Houston, Texas; *Geophysics* **59** 1713–1728.

Norton I O and Sclater J G 1979 A model for the evolution of the Indian Ocean and the breakup of Gondwanaland; *J. Geophys. Res.* **84** 6803–6830.

Pareek H S 1987 Petrographic, chemical and trace elemental composition of the coal of Sohagpur coalfiled, Madhya Pradesh, India; *Int. J. Coal. Geol.* **9** 187–207.

Peter Cary 2006 Reflections on the Deconvolution of Land Seismic Data; CSEG RECORDER , Special Edition.

Raja Rao C S 1983 Coal fields of India Vol-III Coal resources of Madhya Pradesh and Jammu and Kashmir; *Bull. Geol. Surv. India Series* **A45** 204.

Rao G V and Rao R U M 1983 Heat flow in the Indian Gondwana basins and heat production of their basement rocks; *Tectonophys.* **91** 105–117.

Reeves C and de Wit M 2000 Making ends meet in Gondwana: Retracing the transforms of the Indian Ocean and reconnecting continental shear zones; *Terra Nova* **12** 272–280.

Reeves C V, de Wit M J and Sahu B K 2004 Tight reassembly of Gondwana exposes Phanerozoic shears in Africa as global tectonic players; *Gondwana Res.* **7** 7–19.

Riley T R and Knight K B 2001 Age of pre-break-up Gondwana magmatism; *Antarct. Sci.* **13** 99–110.

Sarkar R K and Singh O P 2005 A note on the heat flow studies at Sohagpur and Raniganj coalfiled areas, India; *Acta Geophysica Polonica* **53** 197–204.

Senthil Kumar P and Reddy G K 2004 Radio elements and heat production of an exposed Archaean crustal cross-section, Dharwar craton, south India; *Earth Planet. Sci. Lett.* **224** 309–324.

Senthil Kumar P, Rajeev Menon and Reddy G K 2007a Crustal geotherm in southern Deccan basalt province, India: The Moho is as cold as adjoining cratons; In: Plates, Plumes, and Planetary Processes (eds) Foulger G R and Jurdy D M, *Geol. Soc. Am. Spec. Paper* **430** 275–284, doi: 10.1130/2007.2430(14).

Senthil Kumar P, Rajeev Menon and Reddy G K 2007b The role of radiogenic heat production in the thermal evolution of a Proterozoic orogenic belt: Eastern Ghats,

Indian Shield; *Earth Planet. Sci. Lett.* **254** 39–54, doi: 10.1016/2006.11.018.

Senthil Kumar P, Rajeev Menon and Reddy G K 2009 Heat production heterogeneity of the Indian crust beneath the Himalaya: Insights from the northern Indian Shield; *Earth Planet. Sci. Lett.* **283** 190–196, doi: 10.1016/2009.04.015.

Sheriff R E 1991 Encyclopedic Dictionary of Exploration Geophysics; 3rd edn, *Soc. Explor. Geophys*, 148p.

Sheth H C, Ray J S, Ray R, Vanderkluysen L, Mahoney J J, Kumar A, Shukla A D, Das P, Adhikari S and Jana B 2009 Geology and geochemistry of Pachmarhi dykes and sills, Satpura Gondwana Basin, central India: Problems of dyke-sill-flow correlations in the Deccan Traps; *Contrib. Mineral. Petrol.* **158** 357–380.

Sundaram M S 2007 Methane to markets (M2M) conference on advancing project development in India through public private partnership, New Delhi; http://www.globalmethane.org/documents/events_coal_20070222_22feb07-sundaram.pdf.

Tselentis G A and Paraskevopoulos P 2002 Application of a high-resolution seismic investigation in a Greek coal mine; *Geophysics* **67** 50–59.

Veevers J J 2009 Palinspastic (pre-rift and -drift) fit of India and conjugate Antarctica and geological connections across the suture; *Gondwana Res.* **16** 90–108.

Veevers J J and Tewari R C 1995 Gondwana master basin of peninsular India between Tethys and the interior of the Gondwanaland Province of Pangea; *Geol. Soc. Am. Memoir* **187** 1–73.

Vincent P D, Tsoflias G P, Sleeples D W and Sloan S D 2006 Fixed-source and fixed-receiver walkaway seismic noise tests: A field comparison; *Geophysics* **71** 41–44.

Widess M B 1973 How thin is a thin bed? *Geophysics* **38** 1176–1180.

Ziolkowski A and Lerwill W E 1979 A simple approach to high resolution seismic profiling for coal; *Geophys. Prosp.* **27** 360–394.

MS received 7 September 2012; revised 23 May 2013; accepted 29 May 2013